

# Integrating interactive effects of chilling and photoperiod in phenological process-based models. A case study with two European tree species: *Fagus sylvatica* and *Quercus petraea*



J. Gauzere<sup>a</sup>, S. Delzon<sup>b</sup>, H. Davi<sup>c</sup>, M. Bonhomme<sup>d</sup>, I. Garcia de Cortazar-Atauri<sup>e</sup>, I. Chuine<sup>a,\*</sup>

<sup>a</sup> CNRS, UMR 5175 CEFE, F-34293 Montpellier, France

<sup>b</sup> INRA, UMR 1202 BIOGECO, F-33612 Cestas, France

<sup>c</sup> INRA, UR 0629 URFM, F-84914 Avignon, France

<sup>d</sup> Université Clermont Auvergne, INRA, PIAF, F-63000 Clermont-Ferrand, France

<sup>e</sup> INRA, US 1116 AGROCLIM, F-84914 Avignon, France

## ARTICLE INFO

### Keywords:

Budburst  
Growth competence  
Process-based model  
Dormancy  
Climate change  
Photosensitive species

## ABSTRACT

Modeling studies predict that global warming might severely affect bud dormancy release. However, growing empirical evidences suggest that long photoperiod might compensate for a lack of chilling temperature in photosensitive species. For now, attempts to integrate this effect into models remain limited. Here, we used French budburst phenological records for two main European temperate tree species, *Fagus sylvatica* ( $n = 136$ ) and *Quercus petraea* ( $n = 276$ ), to compare four phenological models accounting for a photoperiod effect, two of them proposing a new formalism of the effect of photoperiod, and three classical thermal models. We also investigated the effect of a realistic photoperiod cue on budburst dates in future climatic conditions. Consistently with the empirical literature, we find that models integrating a photoperiod cue were more relevant to simulate budburst dates for beech than for oak. However, contrary to the recently debated expectation that photoperiod might mitigate the trend towards earlier budburst date, we find that the compensatory effect of photoperiod on a lack of chilling maintains a trend towards earlier dates up to the end of the 2100. Our results also suggest that phenological rank changes between photosensitive and photo-insensitive species may be more pronounced at cold than warm trailing edge.

## 1. Introduction

In the current context of climate change, increasing evidences of species advancing their phenology to track earlier favorable growing season are reported (Root et al., 2003; Berteaux et al., 2004; Menzel et al., 2006). This response is mostly due to phenotypic plasticity (Berteaux et al., 2004; Anderson et al., 2012; Franks et al., 2014). Being able to predict the plastic response of phenological events with climate is therefore of main importance to understand the abilities of species to adapt through phenotypic plasticity to climate change. For sessile, long-lived species, such as trees, this issue is even more critical, as such species may not be able to migrate quick enough to track the shift of their climatic niche (Savolainen et al., 2007; Nathan et al., 2011; Delzon et al., 2013). Another challenge consists in predicting the effect of climate change on the vegetative season length and thus on carbon sequestration and forest productivity (Leinonen and Kramer, 2002; Piao et al., 2008). However, our ability to accurately predict the response of

phenological events in future climatic conditions is frequently challenged (Körner and Basler, 2010; Chuine et al., 2010, 2016). To increase prediction robustness, models notably need to implement the effect of climatic variables on phenology through physiological mechanisms.

Because of its critical role in determining the length of the vegetative season and consequently the annual carbon sequestration (Chen et al., 1999), the date of leaf emergence is one of the phenological trait for which the broader empirical knowledge has been gathered. Consensually, we know that bud growth is mainly triggered by spring warm temperatures (also called forcing temperatures) during a so-called ecodormancy phase (Robertson, 1968; Lang et al., 1987). For temperate perennial species, bud development is preceded by an endodormancy phase (or real dormancy), during which buds are unable to resume growth, even under favorable environmental conditions. This obligatory dormant phase is classically assumed to be an adaptive process protecting buds against frost damages (Howe et al., 1999).

\* Corresponding author at: CEFE, 1919 route de Mende, F-34293 Montpellier cedex 05, France.  
E-mail address: [isabelle.chuine@cefe.cnrs.fr](mailto:isabelle.chuine@cefe.cnrs.fr) (I. Chuine).

Therefore, for most temperate tree species, in normal climatic conditions, buds need to experience some cold temperatures (or chilling temperatures) to release endodormancy.

For more than thirty years, process-based models integrating empirical knowledge of the environmental determinism of phenology have been developed to predict budburst or leaf unfolding and flowering dates. The models commonly used for tree species are (i) models describing the cumulative effect of forcing temperatures on bud development during the ecodormancy phase and (ii) models describing the sequential and cumulative effect of chilling and forcing temperatures on bud development during the endo- and ecodormancy phases respectively. These models have proven their efficiency to explain the current temporal and spacial variation of budburst dates (Vitasse et al., 2011; Basler, 2016). However, counter-intuitively, models simulating only the ecodormancy phase often present similar or higher efficiencies than models simulating both the endo- and ecodormancy phases to predict budburst, while they integrate less biological realism (Linkosalo et al., 2006; Vitasse and Basler, 2013). Many authors argued that this result traduces the fact that the fulfillment of chilling requirements is not a limiting factor under current climatic conditions (e.g. Vitasse and Basler, 2013). Another hypothesis that may explain this result is that the effect of chilling on bud development is not accurately simulated (e.g. Linkosalo et al., 2006).

Recent empirical literature is actually questioning the sequential view of the bud development process (Cooke et al., 2012). Indeed, if the bud endodormancy state is absolute, then we should be able to qualitatively define the end of the endodormancy phase and a dormancy break date. To investigate bud endodormancy, studies often used cutting experiments, in which stems sampled in the field at different dates during the endodormancy phase (autumn–winter) are placed in controlled favorable conditions (growth chamber experiments; Vitasse and Basler, 2014; Dantec et al., 2014). These studies highlighted the difficulties to empirically characterize the dormancy state in most tree species (Zohner and Renner, 2015). Moreover, they showed that the effect of chilling and forcing on bud development are often interactive (e.g. high chilling exposure reduced forcing requirements; Heide, 1993; Caffarra and Donnelly, 2011; Laube et al., 2014; but see Fu et al. (2016)), which supports that the two processes might overlap. Therefore, Cooke et al. (2012) recently argued for a dormancy continuum point of view, similarly to the one described for seeds (Baskin and Baskin, 2004).

Another current debate is questioning the role of photoperiod in bud development. For late-successional species, photoperiod is expected to be a reliable environmental cue to avoid early budburst with fluctuating year-to-year temperatures (Basler and Körner, 2012; Laube et al., 2014). While the major role of the photoperiod on bud set has been demonstrated for most tree species (Howe et al., 2003), no consensus exists about its implication on budburst. Indeed, an increasing body of literature is reporting the effect of photoperiod on budburst, but this effect is often not consistent among studies (Caffarra and Donnelly, 2011; Basler and Körner, 2012, 2014; Laube et al., 2014; Zohner and Renner, 2015; Zohner et al., 2016). These inconsistencies might be due to confusing effects in cutting experiments (as stated by Zohner and Renner, 2015). For instance, buds sampled at different time in natural populations both experienced different chilling and day length. For the species for which the photosensitivity has been clearly demonstrated (e.g. *Fagus sylvatica*, *Betula pubescens*), a consistent photoperiod effect has been seen on insufficiently chilled buds. In that case, increased day length conducted buds to flush earlier at a given forcing temperature. Unfulfilled chilling requirements can thus be compensated by long-day photoperiod (Caffarra and Donnelly, 2011; Zohner and Renner, 2015). Although the effect of photoperiod as a major cue of spring phenology is controversial, its importance might nevertheless increase with global warming and the reduction of chilling temperatures (Körner and Basler, 2010).

In parallel, process-based models need to be adjusted to account for

both the facts that (i) the endodormancy phase may be a more continuous process than once thought, and, (ii) chilling and photoperiod may play a compensatory role in the release of the endodormancy and start of growth in ecodormancy phase. Overlapping models considering the interactive effect of chilling and forcing requirements are now commonly used (Vitasse et al., 2011; Pope et al., 2014; Basler, 2016). The photoperiod effect, first unsuccessfully integrated as a substitute for chilling (Kramer, 1994; Schaber and Badeck, 2003), has recently been included in a complex and dynamic model that accounts for the interactive effect of chilling and photoperiod on bud response to forcing temperatures (Caffarra et al., 2011). While empirical studies are still disentangling the relative importance and interaction of environmental cues in bud development, joint experimental and model improvements is useful. Notably, because of the difficulty of bud cuttings experiments to properly disentangle complex environmental effects, models integrating a photoperiod effect could inform about the role of day length in bud development for species for which this effect is still debated (Vitasse and Basler, 2013; Way and Montgomery, 2015; Basler, 2016; Lange et al., 2016).

Although they often perform equally to simulate current budburst date variation, models that simulate or not the bud endodormancy phase can produce highly divergent predictions in future climatic conditions. Notably, for some tree species and localities, models simulating both the endo- and ecodormancy phases predicted a stagnation of budburst advancement with increasing climate change due to unfulfilled chilling requirements (Morin et al., 2009; Chuine et al., 2016). Many authors argued that for photosensitive species the trend towards budburst stagnation after a certain level of global warming should be reinforced, because of a photoperiod threshold (genotype dependent) that should prevent too early bud development (Körner and Basler, 2010; Vitasse and Basler, 2013). However, considering the endodormancy phase as a quantitative process may attenuate the simulated budburst stagnation since there will be no more an absolute ecodormancy state to reach. Overall, highest complexity behind mechanisms underlying bud development (as chilling-photoperiod interaction) is expected to generate even more complex, non-linear, response of budburst dates with climate change (Lange et al., 2016).

Here, we aimed at investigating the role of chilling and photoperiod on bud development through a modeling approach. To that purpose we compared seven different phenological models accounting for different environmental factors and interactive effects. We tested these models on two major European tree species, *Fagus sylvatica* L. and *Quercus petraea* (Matt.) Liebl. While for *F. sylvatica* empirical studies clearly highlighted a high photoperiod sensitivity (Caffarra and Donnelly, 2011; Basler and Körner, 2012, 2014; Zohner and Renner, 2015), for *Q. petraea*, a few studies reported a slight photoperiod effect (Basler and Körner, 2012, 2014). Therefore, we expect that models including a photoperiod effect to perform better for *F. sylvatica* than *Q. petraea*. To improve the biological realism of phenological modeling, we proposed new models including an interactive effect between chilling and photoperiod on the forcing response through a growth competence function, that traduces the bud ability to accumulate forcing units, as proposed by Hänninen (1990). To calibrate and validate the different phenological models, we used budburst and climatic data sets from observation sites in France. Then we used an external validation procedure to evaluate the performances of the models to predict budburst dates. Finally, for both species, we simulated budburst dates from 1994 to 2098 to evaluate the effect of the photoperiod on spring phenology delay with climate change.

## 2. Materials and method

### 2.1. Phenological and climatic data

We focused on two major European tree species, *F. sylvatica* and *Q.*

*petraea*. To calibrate and validate spring phenological models, we used budburst observations from the RENECOFOR database (retrieved at <http://www.gdr2968.cnrs.fr/>) and from a long-term monitoring in the Pyrénées valleys (Vitasse et al., 2009) covering a large range of latitudinal and elevational variation in France. These observations were consistent in the protocol, i.e. the phenological stage followed was stage 9 on the BBCH scale (Meier, 2001), evaluation of the phenological stage was done individually at the scale of the entire tree crown. More precisely, we used a total of 136 budburst observations, spreading over 16 sites (from the RENECOFOR database only) from 1997 to 2009, for *F. sylvatica*, and 276 observations, spreading over 34 sites (20 from the RENECOFOR database + 14 from Pyrénées valleys) from 1992 to 2014, for *Q. petraea* (Appendix A).

Daily weather data were obtained from ONF databases and climate stations (HOBO Pro RH/Temp, Onset Computer Corporation, Bourne, MA 02532) at the same position than the observation sites. Day length was calculated according to the latitude of the meteorological stations (see Caffarra et al., 2011).

## 2.2. Phenological models

We used seven different models to simulate the budburst dates. To be comparable, all these models use the same mathematical functions to describe the response of bud development to chilling and forcing temperatures. Models differ solely in the way they integrate the effects of chilling accumulation and photoperiod on the ability of bud to accumulate forcing units. In the following, we first describe the chilling and forcing response functions, then we present the models by complexity order. Note that the models do not simulate the endodormancy induction and thus assume that the endodormancy phase has been fully induced.

Based on experimental results obtained on different tree species (Caffarra, 2007), and with a view to simplification, we chose to define the response to chilling temperatures, also called **rate of chilling**  $R_c$ , as a simple threshold function:

$$R_c(T_d) = \begin{cases} 1 & \text{if } T_d < T_b \\ 0 & \text{if } T_d \geq T_b \end{cases} \quad (1)$$

with  $T_d$ , the mean temperature of day  $d$  and  $T_b$ , the threshold temperature (also called base temperature) of the function.

According to Hanninen et al. (1990) and Caffarra and Donnelly (2011), we defined the response to forcing temperatures ( $T_d$ ), also called **rate of forcing**  $R_f$ , as a sigmoid function:

$$R_f(T_d) = \frac{1}{1 + e^{-d_T(T_d - T_{50})}} \quad (2)$$

with  $d_T$  the positive slope and  $T_{50}$  the mid-response temperature of the sigmoid function.

In all models,  $t_0$  defines the beginning of the endo- or eco-dormancy phase depending on the model,  $t_f$  the budburst date and  $F^*$  the critical amount of forcing units to reach budburst.

**UNIFORC** – The UniForc model is an one-phase model, describing the cumulative effect of forcing temperatures on bud development during the ecodormancy phase (Chuine et al., 1999). Budburst occurs when the accumulated  $R_f$  (Eq. (2)) reaches  $F^*$ :

$$\sum_{t_0}^{t_f} R_f(T_d) \geq F^* \quad (3)$$

This model thus assumes that the endodormancy phase has been fully released and that there is no dynamic effects of chilling and photoperiod on forcing requirements. As defined here, the UniForc model has 4 parameters ( $t_0$ ,  $d_T$ ,  $T_{50}$ ,  $F^*$ ). While this model is not biologically relevant for the two studied species, for which a bud dormancy has been experimentally characterized (Basler and Körner, 2012, 2014; Zohner and Renner, 2015), it is still interesting to compare

biologically realistic models with this simpler forcing model to interpret differences in model behaviors.

**UNICHILL** – The UniChill model is a sequential two-phases model describing the cumulative effect of chilling temperatures on bud development during the endodormancy phase (first phase) and the cumulative effect of forcing temperatures during the ecodormancy phase (second phase; Chuine et al., 1999). The end of the endodormancy phase,  $t_c$ , occurs after the accumulated  $R_c$  (Eq. (1)) reaches a critical sum of chilling units,  $C^*$ :

$$\sum_{t_0}^{t_c} R_c(T_d) \geq C^* \quad (4)$$

From  $t_c$  to  $t_f$ , forcing units are then accumulated as:

$$\sum_{t_c}^{t_f} R_f(T_d) \geq F^* \quad (5)$$

This model thus does not describe the compensatory effects of chilling on forcing requirements, neither the effect of photoperiod. The UniChill model has 6 parameters ( $t_0$ ,  $T_b$ ,  $C^*$ ,  $d_T$ ,  $T_{50}$ ,  $F^*$ ).

**UNIFIED** – The UniFied model is an overlapping model, i.e. phases can overlap according to the parameters adjusted, both considering the cumulative effect of chilling and forcing temperatures (Chuine et al., 1999). This model accounts for the compensatory effect of chilling requirements on forcing requirements, with  $F^*$  depending on the total accumulation of chilling units until a date  $t_c$ ,  $C_{tot}$ :

$$F^* = w e^{k C_{tot}}, \quad (6)$$

with  $w > 0$ ,  $k < 0$ , and

$$\sum_{t_0}^{t_c} R_c(T_d) = C_{tot} \quad (7)$$

Forcing units are accumulated from a date  $t_1$ , defined as the day when a critical amount of chilling units  $C^*$  has been reached:

$$\sum_{t_1}^{t_f} R_f(T_d) \geq F^* \quad (8)$$

with

$$\sum_{t_0}^{t_1} R_c(T_d) = C^* \quad (9)$$

In this model the effect of photoperiod is neglected. The UniFied model has 8 parameters ( $t_0$ ,  $T_b$ ,  $C^*$ ,  $t_c$ ,  $w$ ,  $k$ ,  $d_T$ ,  $T_{50}$ ).

**PHOTOTHERMAL** – The Photothermal-time model is an one-phase model, describing the combined effect of chilling, photoperiod and forcing on bud development, first developed for crops and annual plants (Masle et al., 1989; Burghardt et al., 2015). The daily response to photoperiod,  $R_p$ , is described by a sigmoid function:

$$R_p(P_d) = \frac{1}{1 + e^{-d_p(P_d - P_{50})}} \quad (10)$$

with  $P_d$  the photoperiod of the day  $d$ ,  $d_p$  the positive slope and  $P_{50}$  the mid-response parameter of the sigmoid function.

The daily states of photoperiod and forcing, as well as chilling accumulation, are then combined through a multiplicative function to define the photothermal units for budburst,  $R_{tot}$ :

$$R_{tot}(T_d, P_d) = \min\left(\frac{CS(t)}{C^*}, 1\right) R_p(P_d) R_f(T_d) \quad (11)$$

with  $C^*$  the critical amount of chilling accumulation and

$$CS(t) = \sum_{t_0}^t R_c(T_d) \quad (12)$$

Budburst then occurs when:

$$\sum_{t_0}^{t_f} R_{\text{tot}}(T_d, P_d) \geq F^* \quad (13)$$

The Photothermal model has 8 parameters ( $t_0$ ,  $C^*$ ,  $F^*$ ,  $T_b$ ,  $d_p$ ,  $P_{50}$ ,  $d_T$ ,  $T_{50}$ ).

**DORMPHOT1P** – The original Dormphot model is a two-phases model developed by Caffarra et al. (2011) to simulate the paradormancy phase (first phase) and the endo- and ecodormancy phases (treated as a single second phase) accounting for the complex and dynamic effects of chilling and photoperiod on bud dormancy and development. Here, we modified this model by removing the paradormancy phase, to derive a model comparable with the other tested models.

In this one-phase model, the compensatory effect between chilling and photoperiod on bud development is described by a relationship between the daily sum of chilling units, CS, and mid-response photoperiod,  $P_{50}$ , bound between 0 and 24 h, as:

$$P_{50}(\text{CS}) = \frac{24}{1 + e^{-d_C(\text{CS}(t) - C_{50})}} \quad (14)$$

with  $C_{50}$  the mid-response chilling accumulation,  $d_C$  the negative slope of the sigmoid function and

$$\text{CS}(t) = \sum_{t_0}^t R_c(T_d) \quad (15)$$

$P_{50}$  then defines the mid-response parameter of a second sigmoid function that links the photoperiod of day  $d$ ,  $P_d$ , to the mid-response temperature of the forcing response,  $T_{50}$ , bound between 0 and 60 °C, as:

$$T_{50}(P_d) = \frac{60}{1 + e^{-d_p(P_d - P_{50})}} \quad (16)$$

with  $d_p$  the positive slope of the sigmoid function.

We kept the same bounds for the  $P_{50}$  and  $T_{50}$  functions as the one proposed by Caffarra et al. (2011) for *B. pubescens* because of lack of knowledge for the two studied species.

Finally, the rate of forcing,  $R_f$ , dynamically depends on the state of chilling and photoperiod as:

$$R_f(T_d) = \frac{1}{1 + e^{-d_T(T_d - T_{50})}} \quad (17)$$

with  $d_T$  the positive slope of the sigmoid function.

Budburst finally occurs when:

$$\sum_{t_0}^{t_f} R_f(T_d) \geq F^* \quad (18)$$

The Dormphot1P model has 7 parameters ( $t_0$ ,  $F^*$ ,  $T_b$ ,  $C_{50}$ ,  $d_C$ ,  $d_p$ ,  $d_T$ ).

**PGC** – The PGC model (for “Photoperiod effect through Growth Competence function”) is a new model which derives from the Dormphot1P formalism of the compensatory effect between chilling and photoperiod, but integrates this effect through a growth competence function (as proposed by Hänninen, 1990). More precisely, this model considers that the state of chilling and the photoperiod determine the sensitivity of buds to accumulate forcing units, instead of considering that these cues directly affect the forcing response, as in the Dormphot1P model.

This one-phase model also firstly links the state of chilling to the mid-response photoperiod,  $P_{50}$ , with the similar formalism than the Dormphot1P model, but here  $P_{50}$  is bound between  $(12 - P_r)$  and  $(12 + P_r)$  (instead of  $[0; 24]$  in the Dormphot1P model):

$$P_{50}(\text{CS}) = (12 - P_r) + \frac{2P_r}{1 + e^{-d_C(\text{CS}(t) - C_{50})}} \quad (19)$$

with  $P_r$  the range boundaries around 12 h of the parameter  $P_{50}$  and  $d_C$  the negative slope of the sigmoid function, and

$$\text{CS}(t) = \sum_{t_0}^t R_c(T_d) \quad (20)$$

$P_{50}$  then dynamically defines the mid-response parameter of a sigmoid function that links day length,  $P_d$ , to the state of the growth competence:

$$\text{GC}(P_d) = \frac{1}{1 + e^{-d_p(P_d - P_{50}(t))}} \quad (21)$$

with  $d_p$  the positive slope of the sigmoid function.

Finally, the daily state of growth competence modulates the rate of forcing through a multiplicative function, to define the actual daily forcing units accumulated by the buds until budburst as:

$$\sum_{t_0}^{t_f} (\text{GC}(P_d) R_f(T_d)) \geq F^* \quad (22)$$

The PGC model has 9 parameters ( $t_0$ ,  $F^*$ ,  $T_b$ ,  $C_{50}$ ,  $P_r$ ,  $d_C$ ,  $d_p$ ,  $d_T$ ,  $T_{50}$ ).

**PGCA** – The PGC Additive model is a new one-phase model describing the interplay between chilling and photoperiod as an additive effect. The daily chilling accumulation (CS) and photoperiod responses ( $R_p$ ) directly define the growth competence of buds (GC), as:

$$\text{GC}(T_d, P_d) = \min\left(\frac{\text{CS}(t)}{C^*} + R_p(P_d), 1\right) \quad (23)$$

with  $T_d$  and  $P_d$  the temperature and the photoperiod of the day,  $C^*$  the critical amount of chilling accumulation and

$$\text{CS}(t) = \sum_{t_0}^t R_c(T_d) \quad (24)$$

$$R_p(P_d) = \frac{1}{1 + e^{-d_p(P_d - P_{50})}} \quad (25)$$

with  $d_p$  and  $P_{50}$  the positive slope and mid-response photoperiod parameters of the sigmoid function.

As in the PGC model, the daily state of growth competence then modulates the rate of forcing until budburst as:

$$\sum_{t_0}^{t_f} (\text{GC}(T_d, P_d) R_f(T_d)) \geq F^* \quad (26)$$

The PGCA model has 8 parameters ( $t_0$ ,  $F^*$ ,  $T_b$ ,  $C^*$ ,  $d_p$ ,  $P_{50}$ ,  $d_T$ ,  $T_{50}$ ).

While the Photothermal and Dormphot1P models are derived from previously published models, the PGC and PGCA models are new. All these models have been developed to reproduce the empirical results showing that increasing day length conducts buds to flush earlier, i.e. to accumulate faster forcing units at a given temperature in photosensitive species (Caffarra and Donnelly, 2011; Zohner and Renner, 2015). In the Dormphot1P model this effect is represented through an effect of chilling and photoperiod on the mid-response temperature of the forcing response, while in the Photothermal, PGC and PGCA models, this effect is modeled through a growth competence function. In the Dormphot1P and PGC models, the effect of chilling on forcing requirements is indirect, i.e. it goes through the photoperiod response, while in the Photothermal and PGCA models the chilling accumulation directly affects the growth competence. However, in the Photothermal model, budburst can not occur if the bud receives no chilling ( $\text{CS} = 0$ ), which is not in agreement with some experimental observations (Caffarra and Donnelly, 2011).

### 2.3. Calibration and validation

We first used a subset of the data to adjust the model parameters and evaluate the efficiency of the models to explain the observed budburst dates variation. More precisely, we used 97 of the 136 stations for *F. sylvatica* and 175 of the 276 stations for *Q. petraea* to perform the model calibration (a randomly chosen subset of the RENECOFOR data

for both species and all the Pyrenees data for *Q. petraea* to balance the data sets). To facilitate the parameter optimisation (i.e. avoid local optimums) and increase the biological realism of the process-based phenological models, we used empirical results to bind some parameter values (Appendix B). For the two species,  $t_0$  was bound between the 1st September and 1st November for the models simulating both the endo- and ecodormancy phases and  $t_0$  was bound between the 1st December and 1st April for the model simulating only the ecodormancy phase (UniForc model). For the Photothermal, PGC and PGCA models, we also bound the shape parameters of the reaction norms to photoperiod ( $R_p$  and  $GC$  functions) to constrain the photoperiod response to occur at realistic day length values in the latitudes of the studied sites (Appendix B). For *F. sylvatica*, for which we have the best empirical knowledge about the environmental cues affecting bud development, the parameters of the chilling and forcing responses were also bound, mostly according to Caffarra and Donnelly (2011) and Heide and Prestrud (2005) (Appendix B). Note that these restrictions on the parameter space cannot affect the model comparison since all the models are similarly affected. The models were adjusted 20 independent times by minimizing the residual sum of square, using the simulated annealing algorithm of Metropolis (Chuine et al., 1998). To perform the following analyses, we chose the more likely parameter set among these 20 ones, based on the performance to simulate budburst variation in the calibration data set, but also the relevance of the adjusted reaction norms. Indeed, as pointed out by Chuine et al. (2016), statistical inferences can produce statistically equivalent parameter sets that can differ in their biological realism, so that an empirical expertise is often required to select the best parameter adjustment.

We assessed the robustness of the models to accurately predict budburst dates in other sites than the one used for calibration. To perform this external validation, we simulated the budburst dates on the remaining 39 stations for *F. sylvatica* and 101 stations for *Q. petraea*.

The calibration and validation of the models were performed using the Phenological Model Platform software (PMP5; <http://www.cefe.cnrs.fr/fr/ressources/logiciels?id=921>; Chuine et al., 2013). The models were compared using four performance indices: the efficiency ( $EFF$ ), the root mean square error ( $RMSE$  or  $RMSEP$  for the calibration and validation data sets respectively), bias ( $\theta$ ) and corrected Aikake information criterion ( $AIC_c$ ):

$$EFF = 1 - \frac{\sum_{i=1}^n (O_i - P_i)^2}{\sum_{i=1}^n (O_i - \bar{O})^2}, \quad \text{with } EFF \in [-\infty; 1]$$

$$RMSE \text{ or } RMSEP = \sqrt{\frac{\sum_{i=1}^n (O_i - P_i)^2}{n}}$$

$$\theta = \frac{\sum_{i=1}^n (O_i - P_i)}{n}$$

$$AIC_c = N \times \ln\left(\frac{SS_{res}}{n}\right) + 2k + \frac{2k(k+1)}{n-k-1}$$

with  $O_i$  the observation at site  $i$ ,  $\bar{O}$  the average observation value,  $P_i$  the prediction at site  $i$ ,  $n$  the number of observations,  $k$  the number of parameters and  $SS_{res}$  the residual sum of squares of a given model.

The models were also compared according to the biological realism of their adjusted reaction norms. Indeed, a critical analysis of the realism of the adjusted parameter sets is required when comparing the performances and behavior of different models, particularly when they are used to produce projections in climatic conditions that depart from the current ones (Chuine et al., 2013, 2016).

#### 2.4. Impact of climate change on budburst dates

To assess the divergences among the models in future climatic conditions we used the CERFACS climatic simulation under the A1B scenario at a 8-km resolution. The daily mean temperatures were extracted over the 1952–2098 period for three grid points in France: two sites in the Pyrénées mountain at high (42° 53' N 0° 9' E, 1719 m a.s.l.) and intermediate (42° 58' N 0° 9' E, 1075 m a.s.l.) elevations, where some of our phenological observations come from, and one site at the eastern bound of the Pyrénées mountain (La Massane forest;

42° 29' N 2° 58' E, 497 m a.s.l.), which is at the trailing edge of both species. These sites allow to explore a large climatic variability within the distribution range of both *F. sylvatica* and *Q. petraea*. Note that our aim here was not to provide predictions of future budburst dates but to evaluate how a realistic photoperiod cue can affect budburst response to climate warming.

To compare the models prediction over consistent periods, we realized a breakpoint analysis, using both visual characterization and the R-package “segmented”, to define over the whole 1952–2098 scenario homogeneous historic v.s. future climatic periods in terms of budburst responses to temperature. We selected unique breakpoints for both species and models so that the results could be comparable. Based on this analysis, for each model, we estimated budburst deviation from the average historic dates in future climatic conditions. To explore the uncertainties in model projections in future climatic conditions, we also used the different parameter sets obtained for each model, by repeating 20 times the optimization, to estimate the average budburst date predicted ( $\overline{BB}$ ) and the confidence interval around this date (as  $CI_{\overline{BB}} = 1.96 se$ , assuming a normal distribution; with  $se$  the standard error of the estimates).

### 3. Results

#### 3.1. Models efficiency to simulate budburst dates

Model ranking changed according to the performance index. As there is not perfect or fully integrative performance index, we considered the overall performance of the models. Nevertheless, for both species, the calibration and validation procedures show consistent patterns between models, i.e. models explaining the largest variance in the calibration data sets are also among the most accurate to simulate budburst dates in external conditions (and vice-versa; Tables 1 and 2; Appendix C and D).

For *F. sylvatica*, among the models simulating both the endo- and ecodormancy, those integrating an effect of photoperiod on bud development explain best budburst dates variation (i.e. Photothermal, PGC and PGCA models; Table 1), with the exception of the Dormphot1P model that presents one of lowest calibration performance ( $EFF = 0.35$ ,  $AIC_c = 393.63$ ; Table 1). More precisely, according to most of the performance indices, the PGC model provides the most accurate prediction of budburst dates ( $RMSEP = 6.43$ ) and is the most efficient ( $EFF = 0.50$ ,  $AIC_c = 368.19$ ), despite having the highest number of parameters ( $k = 9$ ; Table 1). The thermal endo-ecodormancy models, i.e. UniChill and UniFied models, show similar performance ( $AIC_{UniChill} = 387.78$  and  $AIC_{UniFied} = 387.62$ ; Table 1), while the latter integrate an interactive effect between chilling and forcing requirements. Moreover, these two models present lower overall performance than the thermal model simulating only the ecodormancy phase (UniForc;  $AIC_c = 379.22$ ,  $RMSEP = 6.11$ ; Table 1). Note that this simpler thermal model, UniForc, and the photothermal endo-ecodormancy models present similar performances.

For *Q. petraea*, the models simulating both the endo- and ecodormancy phases present similar performances ( $EFF = [0.74; 0.76]$ ; Table 2), while the thermal ecodormancy model (UniForc) performs the worst ( $AIC_c = 682.41$ ,  $RMSEP = 7.59$ ; Table 2). Notably, differences between models that account or not for an effect of the photoperiod are far less important than for *F. sylvatica*, but models integrating this effect are still among the models that explain the largest proportion of variance in the observations ( $EFF = 0.76$  and  $AIC_c = 668.75$  and  $668.08$  for PGC and PGCA models respectively; Table 2). Still, if we rank the models, the PGCA model has the best calibration and validation performances ( $AIC_c = 668.08$ ,  $RMSEP = 7.15$ ; Table 2). The UniFied model, accounting for the interactive effect between chilling and forcing requirements, performs better than the sequential non-interactive UniChill model ( $AIC_{UniFied} = 668.72$  and  $AIC_{UniChill} = 680.16$ ; Table 2).

**Table 1**  
Optimization of the parameter values for each model and performance indices on calibration and validation data sets for *F. sylvatica*. *N*: number of observations; *k*: number of parameters.

	UniForc	UniChill	UniFied	Photothermal	Dormphot1P	PGC	PGCA
<i>Parameters</i>	$t_0 = 13$ $F^* = 41.3$ $d_T = 0.06$ $T_{50} = 12.41$	$t_0 = -62$ $C^* = 73.7$ $F^* = 37.3$ $T_b = 13.0$ $d_T = 0.08$ $T_{50} = 13.0$	$t_0 = -62$ $C^* = 72.3$ $t_c = 96$ $T_b = 13.0$ $d_T = 0.08$ $T_{50} = 13.0$ $w = 37.88$ $k = -0.0003$	$t_0 = -97$ $C^* = 2.8$ $F^* = 31.0$ $T_b = 9.5$ $d_p = 40$ $P_{50} = 11.4$ $d_T = 0.29$ $T_{50} = 11.9$	$t_0 = -63$ $F^* = 87.1$ $V_b = 12.4$ $C_{50} = 31$ $d_C = -0.71$ $d_p = 13.15$ $d_T = 0.079$	$t_0 = -65$ $F^* = 13.9$ $T_b = 11.9$ $C_{50} = 153.5$ $P_r = 1.76$ $d_C = -40.0$ $d_p = 0.44$ $d_T = 0.25$ $T_{50} = 10.5$	$t_0 = -63$ $F^* = 21.78$ $T_b = 12.4$ $C^* = 18.3$ $d_p = 40$ $P_{50} = 12.85$ $d_T = 0.16$ $T_{50} = 12.29$
<i>Calibration performances</i>							
<i>N</i>	97	97	97	97	97	97	97
<i>k</i>	4	6	8	8	7	9	8
SStot	8589.9	8589.9	8589.9	8589.9	8589.9	8589.9	8589.9
SSres	4837.7	5283.9	5275.5	4807.8	5612.4	4317.6	4671.2
$\theta$	0.01	-0.05	-0.07	-0.08	-0.05	0.23	0.06
RMSE	7.06	7.38	7.37	7.04	7.61	6.67	6.94
EFF	0.44	0.39	0.39	0.44	0.35	0.50	0.46
AIC <sub>c</sub>	379.22	387.78	387.62	378.62	393.63	368.19	375.82
<i>Validation performances</i>							
<i>N</i>	39	39	39	39	39	39	39
$\theta$	-0.73	-0.34	-0.31	-1.11	-0.68	-0.67	-1.00
RMSEP	6.11	7.75	7.82	6.99	7.43	6.43	6.94

3.2. Adjusted reaction norms to photoperiod

While several models tested here integrate a photoperiod effect, the effective response to day length simulated by the models can highly differ according to the adjusted reaction norms. Note that these reaction norms are the result of a statistical adjustment and might differ from the true ones. As the model performances support a higher photosensitivity for *F. sylvatica* than *Q. petraea*, here we only present the adjusted reactions norms to photoperiod for *F. sylvatica*. But note that the adjusted reaction norms for *Q. petraea* suggest a negligible effect of photoperiod on bud development (either low  $P_{50}$  or  $C^*/C_{50}$ ; Table 2).

The adjusted reaction norms of the Photothermal and PGCA models show a threshold response to the photoperiod, with a mid-response parameter equals to  $P_{50} = 11.40$  h and 12.85 h respectively. Note that the  $P_{50}$  parameter has a slightly different meaning in the two models: for the Photothermal model, it means that only days with more than

11.40 h of day length can be effective to accumulate forcing units. For the PGCA model, it implies that days with at least 12.85 h of day length can fully compensate the lack of chilling requirements. However, the low chilling requirements adjusted for this latter model ( $C^* = 18.3$ ; Table 1) are not expected to be limiting, even in future climatic conditions. For the PGC model, the response to photoperiod is dynamic and the mid-response photoperiod,  $P_{50}$ , varies from 10.24 h to 13.76 h. As the adjusted reaction norms defining the compensatory effect between chilling and photoperiod is a threshold ( $d_C = -40$ ),  $P_{50}$  can actually only take these two values (Fig. 1a). The high chilling requirements adjusted for this model ( $C_{50} = 153.5$ ; Table 1) indicates a higher photoperiod effect on insufficiently chilled buds: below  $C_{50}$  (i.e. less than 153 days below 11.9 °C) long-day lengths ( $P_{50} = 13.76$  h) are required for buds to develop, while above  $C_{50}$  (i.e. more than 153 days below 11.9 °C), buds can develop at shorter day lengths ( $P_{50} = 10.24$  h; Fig. 1c).

**Table 2**  
Optimization of the parameter values for each model and performances indices on calibration and validation data sets for *Q. petraea*. *N*: number of observations; *k*: number of parameters.

	UniForc	UniChill	UniFied	Photothermal	Dormphot1P	PGC	PGCA
<i>Parameters</i>	$t_0 = 55$ $F^* = 26$ $d_T = 0.44$ $T_{50} = 8.30$	$t_0 = -63$ $C^* = 116.7$ $F^* = 23.0$ $T_b = 13.4$ $d_T = 0.41$ $T_{50} = 9.0$	$t_0 = -64$ $C^* = 115.1$ $t_c = 105$ $T_b = 13.2$ $d_T = 0.27$ $T_{50} = 9.0$ $w = 26.19$ $k = -0.0009$	$t_0 = -63$ $C^* = 158$ $F^* = 9.86$ $T_b = 12.4$ $d_p = 25.8$ $P_{50} = 6.33$ $d_T = 0.16$ $T_{50} = 20.4$	$t_0 = -63$ $F^* = 24.8$ $T_b = 14.5$ $C_{50} = 120$ $d_C = -0.16$ $d_p = 19.2$ $d_T = 0.35$	$t_0 = -121$ $F^* = 26.0$ $T_b = 10.7$ $C_{50} = 10.0$ $P_r = 0.92$ $d_C = -0.26$ $d_p = 40$ $d_T = 0.42$ $T_{50} = 8.47$	$t_0 = -106$ $F^* = 15.0$ $T_b = 12.4$ $C^* = 25.8$ $d_p = 16.6$ $P_{50} = 11.95$ $d_T = 0.32$ $T_{50} = 10.3$
<i>Calibration performances</i>							
<i>N</i>	175	175	175	175	175	175	175
<i>k</i>	4	6	8	8	7	9	8
SStot	32,918.4	32,918.4	32,918.4	32,918.4	32,918.4	32,918.4	32,918.4
SSres	8640.94	8530.4	7990.8	8267.4	8269.3	7992.3	7961.4
$\theta$	4.2	0.02	-0.06	0.18	0.07	-0.10	0.35
RMSE	7.03	6.98	6.76	6.87	6.87	6.76	6.74
EFF	0.74	0.74	0.76	0.75	0.75	0.76	0.76
AIC <sub>c</sub>	682.41	680.16	668.72	674.68	674.72	668.75	668.08
<i>Validation performances</i>							
<i>N</i>	101	101	101	101	101	101	101
$\theta$	2.60	-1.73	-1.33	-1.57	-1.07	-1.66	-1.49
RMSEP	7.59	7.36	7.37	7.78	7.16	7.56	7.15

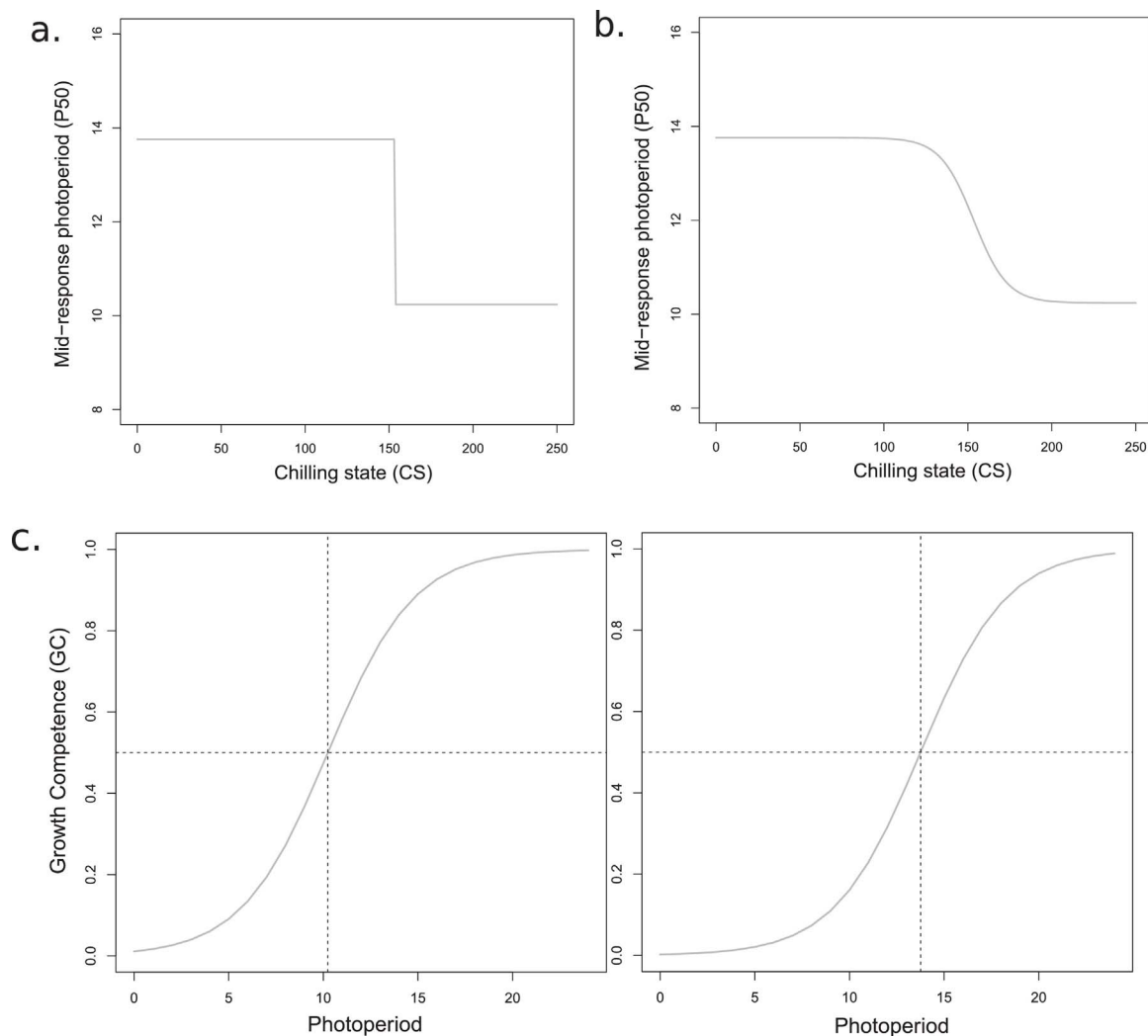


**Fig. 1.** Adjusted reaction norms of the PGC model for *F. sylvatica*. (a) Adjusted relationship between chilling state (CS) and mid-response photoperiod ( $P_{50}$ ). (b) Relationship between CS and  $P_{50}$  using a realistic shape parameter ( $d_C = -0.1$  instead of  $-40$ ). (c) Adjusted relationship between photoperiod and growth competence (GC). The shape of this relationship varies with CS: here the two extreme configurations are represented (i.e. with  $P_{50} = 10.2$  and  $13.8$ ). The dashed line represented the  $P_{50}$  value for which by definition  $GC = 0.5$ .

**Table 3**

Budburst deviations trends (slope in days per decade) predicted by each model for *F. sylvatica* along the climatic gradient from 1994 to 2059 ( $p_A$ ), 2060 to 2098 ( $p_B$ ) and over the whole period (1994–2098;  $p_{A+B}$ ). In brackets are indicated the  $p$ -value of the linear model, with “\*\*\*\*”  $p < 0.001$ , “\*\*\*”  $0.001 < p < 0.01$ , “\*\*”  $0.01 < p < 0.05$ , “.”  $0.05 < p < 0.09$  and “ns”  $p > 0.09$ .

Method	Pyrénées 1719 m			Pyrénées 1075 m			Massane 497 m		
	$p_A$	$p_B$	$p_{A+B}$	$p_A$	$p_B$	$p_{A+B}$	$p_A$	$p_B$	$p_{A+B}$
UniForc	-1.63 <sup>(****)</sup>	-0.32 <sup>(ns)</sup>	-1.18 <sup>(****)</sup>	-1.40 <sup>(****)</sup>	-0.20 <sup>(ns)</sup>	-1.01 <sup>(****)</sup>	-1.08 <sup>(****)</sup>	-0.03 <sup>(ns)</sup>	-0.72 <sup>(****)</sup>
UniChill	-2.04 <sup>(****)</sup>	-0.39 <sup>(ns)</sup>	-1.47 <sup>(****)</sup>	-1.61 <sup>(****)</sup>	0.13 <sup>(ns)</sup>	-1.11 <sup>(****)</sup>	0.26 <sup>(ns)</sup>	0.24 <sup>(ns)</sup>	0.20 <sup>(ns)</sup>
UniFied	-2.02 <sup>(****)</sup>	-0.32 <sup>(ns)</sup>	-1.45 <sup>(****)</sup>	-1.60 <sup>(****)</sup>	0.15 <sup>(ns)</sup>	-1.09 <sup>(****)</sup>	0.26 <sup>(ns)</sup>	0.16 <sup>(ns)</sup>	0.21 <sup>(ns)</sup>
Photothermal	-2.35 <sup>(****)</sup>	-0.61 <sup>(ns)</sup>	-1.70 <sup>(****)</sup>	-1.70 <sup>(****)</sup>	-0.15 <sup>(ns)</sup>	-1.15 <sup>(****)</sup>	-0.84 <sup>(****)</sup>	0.15 <sup>(ns)</sup>	-0.50 <sup>(****)</sup>
Dormphot1P	-1.78 <sup>(****)</sup>	-0.29 <sup>(ns)</sup>	-1.27 <sup>(****)</sup>	-1.24 <sup>(****)</sup>	0.35 <sup>(ns)</sup>	-0.81 <sup>(****)</sup>	0.82 <sup>(.)</sup>	0.42 <sup>(ns)</sup>	0.64 <sup>(****)</sup>
PGC	-2.81 <sup>(****)</sup>	-0.78 <sup>(ns)</sup>	-1.99 <sup>(****)</sup>	-1.76 <sup>(****)</sup>	-0.08 <sup>(ns)</sup>	-1.33 <sup>(****)</sup>	-2.12 <sup>(****)</sup>	-0.32 <sup>(ns)</sup>	-1.48 <sup>(****)</sup>
PGCA	-2.40 <sup>(****)</sup>	-0.75 <sup>(ns)</sup>	-1.74 <sup>(****)</sup>	-1.71 <sup>(****)</sup>	-0.09 <sup>(ns)</sup>	-1.26 <sup>(****)</sup>	-0.25 <sup>(ns)</sup>	0.34 <sup>(ns)</sup>	-0.11 <sup>(ns)</sup>
Average	-2.15	-0.49	-1.54	-1.57	0.02	-1.11	-0.42	0.14	-0.25

Interestingly, the adjusted reaction norms to forcing temperatures are steeper in models integrating a photoperiod effect (except Dormphot1P;  $d_T \in [-0.29; -0.16]$ ) than in classical thermal models ( $d \in [-0.08; -0.06]$ ; Table 1), traducing a higher sensitivity to spring warm temperatures. Note that the low performances and likelihood of the adjusted reaction norms of the Dormphot1P model may be due to the low relevance of the fixed values used as bounds for the  $P_{50}$  and  $T_{50}$  functions.

### 3.3. Budburst projections with climate change

For most of the models, we find two major breakpoints in the predicted budburst trends of both species: 1994 and 2060 (see Appendices E and F). Hereafter, the period from 1952 to 1993 is called the historic period and the period from 1994 to 2098 the future period. Budburst deviations from average historic dates in the current/future climate were always analyzed over the whole 1994–2098 period and,

**Table 4**

Budburst deviations trends (slope in days per decade) predicted by each model for *Q. petraea* along the climatic gradient from 1994 to 2059 ( $p_A$ ), 2060 to 2098 ( $p_B$ ) and over the whole period (1994–2098;  $p_{A+B}$ ). In brackets are indicated the  $p$ -value of the linear model, with “\*\*\*\*”  $p < 0.001$ , “\*\*\*”  $0.001 < p < 0.01$ , “\*\*”  $0.01 < p < 0.05$ , “.”  $0.05 < p < 0.09$  and “ns”  $p > 0.09$ .

Method	Pyrénées 1719 m			Pyrénées 1075 m			Massane 497 m		
	$p_A$	$p_B$	$p_{A+B}$	$p_A$	$p_B$	$p_{A+B}$	$p_A$	$p_B$	$p_{A+B}$
UniForc	-3.83 <sup>(****)</sup>	-1.01 <sup>(ns)</sup>	-2.63 <sup>(****)</sup>	-3.48 <sup>(****)</sup>	-0.14 <sup>(ns)</sup>	-2.31 <sup>(****)</sup>	-1.64 <sup>(****)</sup>	-0.12 <sup>(ns)</sup>	-1.02 <sup>(****)</sup>
UniChill	-3.78 <sup>(****)</sup>	-1.06 <sup>(ns)</sup>	-2.6 <sup>(****)</sup>	-3.48 <sup>(****)</sup>	0.07 <sup>(ns)</sup>	-2.26 <sup>(****)</sup>	-0.15 <sup>(ns)</sup>	1.96 <sup>(*)</sup>	0.35 <sup>(*)</sup>
UniFied	-3.47 <sup>(****)</sup>	-0.99 <sup>(ns)</sup>	-2.41 <sup>(****)</sup>	-3.39 <sup>(****)</sup>	0.12 <sup>(ns)</sup>	-2.22 <sup>(****)</sup>	0.51 <sup>(.)</sup>	2.65 <sup>(*)</sup>	0.83 <sup>(****)</sup>
Photothermal	-3.57 <sup>(****)</sup>	-1.24 <sup>(*)</sup>	-2.51 <sup>(****)</sup>	-3.12 <sup>(****)</sup>	0.19 <sup>(ns)</sup>	-2.12 <sup>(****)</sup>	-0.69 <sup>(.)</sup>	0.68 <sup>(ns)</sup>	-0.28 <sup>(ns)</sup>
Dormphot1P	-5.10 <sup>(****)</sup>	-1.27 <sup>(ns)</sup>	-3.50 <sup>(****)</sup>	-3.70 <sup>(****)</sup>	0.13 <sup>(ns)</sup>	-2.38 <sup>(****)</sup>	-0.45 <sup>(ns)</sup>	1.31 <sup>(.)</sup>	0.12 <sup>(ns)</sup>
PGC	-2.59 <sup>(****)</sup>	-0.57 <sup>(ns)</sup>	-1.59 <sup>(****)</sup>	-3.17 <sup>(****)</sup>	-0.03 <sup>(ns)</sup>	-2.06 <sup>(****)</sup>	-1.42 <sup>(****)</sup>	0.02 <sup>(ns)</sup>	-0.85 <sup>(****)</sup>
PGCA	-4.00 <sup>(****)</sup>	-1.81 <sup>(*)</sup>	-2.77 <sup>(****)</sup>	-3.36 <sup>(****)</sup>	-0.45 <sup>(ns)</sup>	-2.24 <sup>(****)</sup>	-1.20 <sup>(****)</sup>	0.16 <sup>(ns)</sup>	-0.60 <sup>(****)</sup>
Average	-3.76	-1.14	-2.57	-3.39	-0.02	-2.23	-0.72	0.95	-0.21

independently, from 1994 to 2059 and 2060 to 2098.

### 3.3.1. Comparison of model projections over the 1994–2098 period

At the lowest elevation, for both species, UniForc and endo-ecodormancy models accounting for a photoperiod effect both predict budburst advancement over the whole 1994–2098 period (except Dormphot1P) ( $p_{photoperiod} \in [-1.48; -0.11]$  and  $p_{photoperiod} \in [-0.85; -0.28]$  days/decade for *F. sylvatica* and *Q. petraea* respectively; Tables 3 and 4). Contrarily, classical thermal endo-ecodormancy models, UniChill and UniFied, overall predict a stagnation and a slight delay of budburst dates for *F. sylvatica* and *Q. petraea* respectively (Tables 3 and 4). At the highest and intermediate elevations, models integrating a photoperiod effect predict a higher overall advancement than classical thermal models for *F. sylvatica* (except Dormphot1P) ( $p_{PGC} \in [-1.7; -1.99]$ ,  $p_{UniChill} = -1.47$  and  $p_{UniForc} = -1.18$  days/decade at high elevation; Table 3; Fig. 2) while they predict equivalent or lower overall advancement than thermal models for *Q. petraea* (except Dormphot1P) ( $p_{PGC} = [-2.77; -1.59]$ ;  $p_{UniChill} = -2.60$  and  $p_{UniForc} = -2.63$  days/decade at high elevation; Table 4; Fig. 2). For both species and every simulation site, the 2060 breakpoint year marks a strong change in budburst date trends in the future period: for most of the models the budburst advancement drastically decreases after 2060 ( $p_A = -1.38$  and  $p_B = -0.11$  days/decade on average for *F. sylvatica*;  $p_A = -3.24$  and  $p_B = -0.07$  days/decade for *Q. petraea*) and is no more significant. We show that this general change in the shift of budburst date is due a slowdown of the warming of spring temperatures during this period in the climatic scenario used (Appendix G).

### 3.3.2. Higher budburst advancement at high elevations for *Q. petraea*

Focusing on the budburst prediction differences between elevations over the whole period, we can see that for both species, models tend to predict increasing budburst advancement with elevation, with an average  $p = -1.54$  at 1719 m,  $p = -1.11$  at 1075 m and  $p = -0.25$  days/decade at 497 m elevation for *F. sylvatica* (Table 3), and, an average  $p = -2.57$  at 1719 m,  $p = -2.23$  at 1075 m and  $p = -0.21$  days/decade at 497 m elevation for *Q. petraea* (Table 4; Fig. 2). At intermediate and high elevations, the predicted budburst advancements are higher for *Q. petraea* than *F. sylvatica*. However, at the lowest elevation site, budburst advancements are similar between the two species (Tables 3 and 4).

### 3.3.3. Contrasted projections between classical thermal models and models including a photoperiod cue

In the warmest climatic conditions, the pattern of budburst advancement predicted by models with a photoperiod cue for the whole 1994–2098 period, as opposed to the stagnation predicted by classical thermal endo-ecodormancy models such as the UniChill, can appear counter-intuitive. To understand this result, we detailed the state of bud development predicted by the PGC model for *F. sylvatica* at this low

elevation site. Averaging the daily state of bud development over the three climatic periods defined above, we can see that the total amount of chilling units accumulated (CS) decreases from 1952 to 2098 at the warmest site (Appendix H). As the threshold temperature of the chilling response during the endodormancy phase is very similar in the PGC and UniChill models (12 vs 13 °C), CS also decreases for the UniChill model. We can also note that both in the current and future climatic conditions, the critical amount of chilling (i.e. 153 days below 11.9 °C) required to decrease the photoperiod sensitivity ( $P_{50}$ ) is actually never reached in the PGC model (Appendix H). Consequently, the growth competence variation only depends on the photoperiod and thus does not vary between climatic periods (Appendix H). However, during the late-winter and early-spring, the growth competence of the PGC model is never null because of the effect of photoperiod, while it is null in the UniChill model because the critical amount of chilling has not been reached. The increased advancement of budburst date along the 21st century in the PGC projections is thus mainly explained by an increased accumulation of forcing units because of global warming, mostly during the end of winter and spring, when the growth competence is maximal (Appendix H). Exploring the consequences of a more continuous relationship between  $P_{50}$  and CS (Fig. 1b) on the validity of our results by changing the  $d_c$  value ( $d_c = -0.1$ ), we show that despite a decreasing average growth competence over the period, the forcing still accumulates faster because of an increasing climate warming (Appendix H). One needs to note also that the adjusted forcing reaction norm of the PGC model also shows a higher thermal sensitivity (i.e. steeper slope of the sigmoid function) as compared to classical thermal models, which explains why the PGC model tends to predict higher budburst advancement than UniForc. In conclusion, in the PGC model, photoperiod compensates for a large part the decreasing rate of accumulation of chilling and allows bud growth to take place earlier than in the UniChill model, thereby generating much earlier budburst dates.

### 3.3.4. Higher uncertainties for models integrating complex environmental cues

Focusing on the mostly used budburst models for tree species, i.e. UniForc and UniChill, and the PGC model that appeared as the most relevant among the models integrating a photoperiod effect, we found that uncertainties in model predictions increase with model complexity and in marginal climatic conditions (i.e. in current climatic conditions at high elevation and future climatic conditions at low elevation) (Fig. 2; Appendix I). However, the uncertainties are not high enough to erase the differences between models in the predicted budburst trends with climate warming (Fig. 2).

## 4. Discussion

Investigating the factors underlying the bud development process

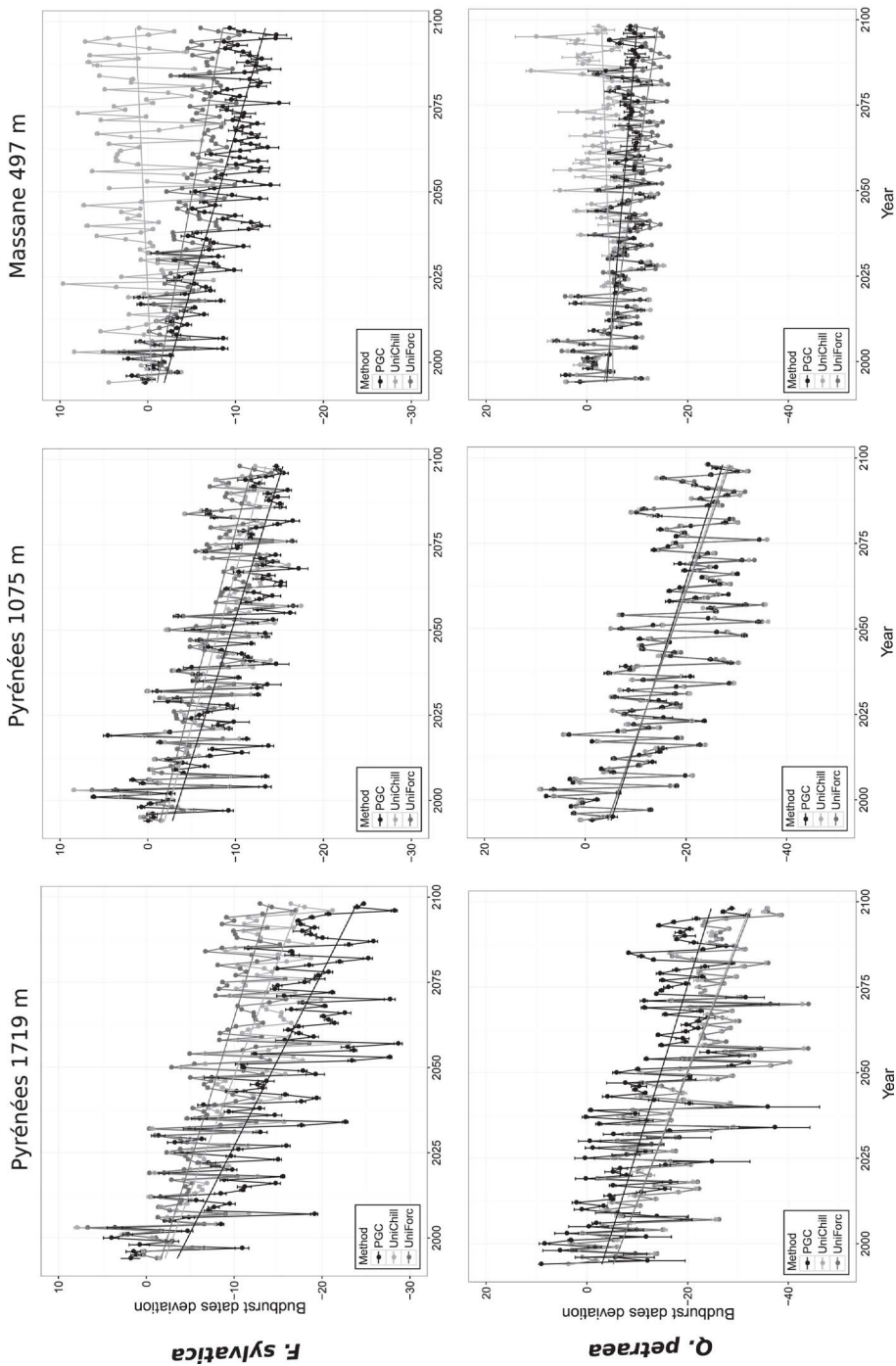


Fig. 2. Uncertainties in the model predictions of budburst deviations from average historic dates (1952–1993) for the period 1994–2098 for *F. sylvatica* (above) and *Q. petraea* (below). We focus on the comparison of the mostly used budburst models for tree species, i.e. the one-phase model “UniForc” (gray) and the two-phases model “UniChill” (light gray), and the “PGC” (black) model, which appeared as the most relevant among the models integrating a photoperiod effect. Black dots are the average budburst dates estimated from the 20 adjustment runs and error bars are the confidence intervals around these estimates. Note that the y-axis has different scales between the two species.

through a modeling approach has several advantages and pitfalls. Among the advantages, model comparison allows to properly disentangle the relative roles of different environmental variables on budburst variation (the more accurate approach being to use nested models accounting for different cues). The main drawback of using complex models to better understand processes and their interaction is the possible problems of overfitting and parameter compensation that can lead to wrong interpretations. For these reasons, the results presented here should be taken with caution and view as insights to orientate future experimental research. Nevertheless, while models with different degree of complexity (in terms of physiological processes they integrate) can present equivalent statistical performances, it is always critical to evaluate the relevance of a model based on the biological realism of the adjusted reaction norms using some empirical expertise (Chuine et al., 2013, 2016).

#### 4.1. Photoperiod sensitivity may not limit budburst advancement

In the literature, many authors argued that the phenology of photosensitive species should be less affected by spatial and temporal climate variations than non-photosensitive, because of their lower thermal sensitivity (Körner and Basler, 2010). An extrapolated conclusion is that models integrating an accurate photoperiodic effect should simulate stronger budburst stagnation than the one predicted by current thermal models. At the opposite, some authors emphasized that, for now, the empirical studies have always showed a predominant role of temperature on bud development suggesting that budburst variation driven by climate change should not be completely concealed by a photoperiod control (Chuine et al., 2010). Overall, and in a more consensual way, we expect the observed effect of global warming on phenology over the last decades to be an inaccurate predictor of the future phenological response because of non-linear response of budburst to climate warming (as the physiological responses to temperature are non-linear; Caffarra and Donnelly (2011)). Indeed, recent evidences showed an ongoing decreasing sensitivity to spring forcing temperatures (resulting in a lowering of budburst dates advancement), likely due to the increasing importance of unfulfilled chilling requirements (Fu et al., 2015b).

The results of our modeling approach suggest that photoperiod plays a significant role in budburst for *F. sylvatica*, but not for *Q. petraea*. Indeed, for *F. sylvatica* only, (i) the inclusion of a photoperiod cue increases substantially the efficiency of the endo-ecodormancy models to explain and predict budburst dates and (ii) the adjusted reaction norms are consistent with a non-negligible effect of photoperiod on bud development. This result is consistent with the higher photoperiod effect detected for *F. sylvatica* as compared to *Q. petraea* in bud cutting experiments (Basler and Körner, 2012, 2014). Over the 1994–2098 period, we also predict a higher budburst advancement for *Q. petraea* than *F. sylvatica*, which is in agreement with lower thermal sensitivity of photosensitive species and is consistent with previous simulation studies (Vitasse et al., 2011).

Our simulations in contrasted climatic conditions do not suggest that models integrating a biologically realistic photoperiod effect tend to predict higher budburst stagnation than classical thermal models. As illustrated in the warmest climatic conditions, since photoperiod compensates the slowing down of chilling rate accumulation, a trend toward budburst advancement can be maintained despite increasing warming temperatures for photosensitive species. Our results are thus in agreement with the common view that southern populations are more affected by photoperiod than northern populations (Vitasse and Basler, 2013) in the sense that a photoperiod effect has a key compensatory role to release bud dormancy in the warmest conditions. However, even in this particular trailing edge condition, our results also support the fact that warming temperatures are still a major driver of budburst date variation, as the forcing model (UniForc) predicts budburst trends in the range of those predicted by models accounting

for a photoperiod effect.

Our results might appear in contradiction with the recent simulation study of Lange et al. (2016), concluding that unfulfilled chilling requirements and increasing dependency on photoperiod may limit future budburst advancement. The authors indeed used a model integrating a photoperiod effect and predicted a lower budburst advancement for the 2002–2100 period as compared to the 1951–2009 period for four temperate tree species, including *F. sylvatica*, but they have not compared their projections with other photoperiod models neither more classical thermal models. Moreover, a recent meta-analysis by Fu et al. (2015b) showed that the decreasing thermal sensitivity of European tree species cannot be easily explained by a photoperiodic constrain, even if the authors do not exclude this hypothesis. More particularly, among the studied species, they showed that *F. sylvatica* was the one with the lowest global thermal sensitivity (over the 1980–2013 period), but also the one for which the change in apparent budburst temperature sensitivity was the lowest (Fu et al., 2015b), which also contradicts the common thought that future budburst advancement should be more limited for photosensitive species.

#### 4.2. Modelling budburst of photosensitive species

Vitasse and Basler (2013) summed up two main ways photoperiod may interact with chilling and forcing temperatures: (1) a fixed photoperiod may be required to accumulate forcing units to a given requirement that is determined by chilling fulfillment; (2) the forcing requirements or the bud sensitivity to forcing temperatures may be affected by a photoperiod increase or a photoperiodic threshold. Among the models including a photoperiod effect, the overall best performances of the PGC model for *F. sylvatica* support hypothesis (2), i.e. photoperiod dynamically affects bud growth competence according to the level of chilling accumulation. The growth competence function, which represents the ability of the bud to accumulate forcing units for a given, unchanged forcing reaction norm, directly describes the continuous state of bud dormancy advocated by Cooke et al. (2012). Our results for *F. sylvatica* show an equivalent performance gain ( $AIC_c$ ) when adding a “simple” modulator threshold photoperiod effect to a thermal model (i.e. Photothermal vs UniChill) than when adding an explicit growth competence function that incorporate the compensatory role between chilling and photoperiod to a photothermal model (i.e. PGC vs Photothermal).

The consistency between the adjusted reaction norms of the PGC model and the current empirical knowledge about bud development for *F. sylvatica* also supports the chilling x photoperiod modeling through a growth competence function. Indeed, the adjusted PGC model simulates a higher impact of photoperiod on insufficiently chilled buds, consistently with Caffarra and Donnelly (2011), Laube et al. (2014), Zohner and Renner (2015). The adjusted forcing reaction norm also shows a higher thermal sensitivity (i.e. steeper slope of the sigmoid function) as compared to classical one- and two-phases models which is consistent with the empirical reaction norm estimated by Caffarra and Donnelly (2011). Finally, the non-null growth competence in late autumn/early-mid-winter, allowing forcing units to be physiologically effective and accumulated during this period, gives rise to the possibility of simulating autumn flushing in spring flushing species, as it is more and more often observed in mild climate ([www.obs-saisons.fr](http://www.obs-saisons.fr)). The growth competence function indeed represents the level of endodormancy, and its dynamics can both simulate dormancy induction and release.

Phenological models for *F. sylvatica* usually show lower efficiency as compared to other temperate tree species (Vitasse et al., 2011). This has been classically explained by the absence of photoperiod cue in models. Despite we find an increased percentage of budburst variance explained by models integrating a photoperiod effect for *F. sylvatica*, we still fail at explaining at least 50% of the remaining variance. Possible and non-exhaustive explanations are that: (1) we still lack a complete under-

standing of the photoperiod  $\times$  chilling interaction on bud growth competence; (2) other abiotic cues have a major influence on *F. sylvatica* budburst phenology (e.g. water availability, air humidity, insolation, temperatures in late summer; Fu et al., 2015a); (3) the spring phenology of this species is more sensitive to biotic conditions than other forest tree species (e.g. resources, parasitism); (4) *F. sylvatica* populations present a stronger genetic differentiation than other species. Nevertheless, the variance in budburst observations for *F. sylvatica* being particularly low, we can not expected the model statistical efficiencies to be in the same range than the one of other temperate tree species.

Our results agree with the previously debated idea of Linkosalo et al. (2006), that simple ecodormancy models can present relatively good performance as compared to more complex endo-ecodormancy models if the effect of environmental cues on bud development are not accurately simulated (UniChill performed worst than UniForc for the photosensitive species *F. sylvatica*). However, in that case the similar performance between UniForc and photothermal models also suggests that the adjustment of models simulating the endodormancy phase is probably challenged in current climatic conditions, as dormancy release is not compromised in these conditions, which provides a higher weight to the ecodormancy driver, the forcing temperatures, in the setting of budburst dates (Vitasse and Basler, 2014). As for classical thermal models, the lack of measurements for the bud endodormancy state probably hampers accurate fit of complex and dynamic photoperiod models (Chuine et al., 2016). There is a strong need for more experimental measurements of bud dormancy continuum and a finest description of the interplay between photoperiod and chilling accumulation on this quantitative state, that can then be used to improve reaction norms description and the adjustment of models. To achieve these aims one of the greatest experimental challenges will notably be to monitor on large samples continuous physiological processes (e.g. measure of the metabolic activity) behind the visible and qualitative bud states (as the ones described by the BBCH scale; Meier, 2001).

#### 4.3. Ecological considerations for warm trailing edges

Phenology is one of the main driver of species distributions (Chuine and Beaubien, 2001). Major phenological changes predicted for the next century may therefore have a strong impact on the redefinition of species range limits and forest community composition. The fate of warm trailing edge populations is notably critical as climate change may generate severe mortality and range contractions (Morin et al., 2008). In addition, changes in phenological rank between photosensitive and photo-insensitive species are expected to be more pronounced in warmest conditions, with photo-insensitive species being more able to track the earlier start of the growing season. This change in the competitive balance between species may therefore accentuate the decline of photosensitive species at the warm trailing edge of their distribution (Vitasse et al., 2011).

Here, using models that include a realistic photoperiod effect, we find that changes in predicted budburst dates over the 1994–2098 period are more similar between species in the warmest conditions than in the coolest, which does not suggest that the competitive balance may disadvantage the photosensitive species *F. sylvatica* at the profit of the photo-insensitive species *Q. petraea*. At the opposite, this suggests that it is at high and intermediate elevations, where the phenological changes will be the most important (consistently with previous simulations studies; Vitasse et al., 2011), that we will find the highest difference in budburst advancement between the two species. Therefore, shifts in phenological rank between photosensitive and photo-insensitive species may more importantly affect the expansion process taking place at the cool leading edges.

Zohner et al. (2016) showed that out of 173 extra-tropical woody species, only 35% rely on spring photoperiod as a leaf-out signal and that these species come from lower latitudes, whereas species from high

latitudes with long winters leaf out independent of photoperiod. According to them, northern woody species evolved photoperiod-independent leaf-out strategies because at high latitudes day-length increase in spring occurs too early for frost to be safely avoided. The authors also conclude that their finding supports the idea that photoperiodism may slow down or constrain poleward range expansion of photosensitive species. Our results suggest, contrarily to Zohner et al. (2016) conclusion, that southern woody species need to rely on a photoperiodic cue in addition to temperature to overcome dormancy break failure due to a lack of chilling temperature. As a consequence, photoperiod sensitivity might help southern species to cope with warmer winters and dormancy break failures, and consequently help them shifting their potential distribution poleward which will however not necessarily translate to a shift in their realized distribution because of dispersal limitations (Saltre et al., 2015).

## 5. Conclusion

The results obtained here suggest that models integrating a compensatory effect of long photoperiod on chilling deficiency are more appropriate to simulate current budburst dates variation in photosensitive species. These conclusions are not only drawn from the comparison of the model statistical performances, but also, and very importantly, from the consistency between the adjusted reaction norms and the current empirical knowledge. Contrarily to the recently debated expectation that photoperiod might conceal the trend towards earlier budburst date, we find that the compensatory effect of photoperiod on a lack of chilling may maintain a trend towards earlier dates up to the end of the 2100. The thermal sensitivity of photosensitive species being less affected by climate warming and the reduction of chilling than the one of photo-insensitive species, phenological rank changes between photosensitive and photo-insensitive species may be more pronounced at cold than warm trailing edges.

## Conflicts of interest

The authors have no conflict of interest to declare.

## Acknowledgments

We are grateful to the ONF and the RENECOFOR network and to Jean-Marc Louvet (INRA Biogeco) for the phenological monitoring. The authors thank the Experimental Unit of Pierroton (UE 0570, INRA, 69 route d'Arcachon, 33612 CESTAS) and Toulence (UE 0393, INRA, Domaine des Jarres, 33210 Toulence) for providing material and logistics. We also thank the three anonymous reviewers for their constructive comments on previous versions of the manuscript. This study was funded by the ANR-13-ADAP-0006 project MeCC.

## Appendix A. Supplementary data

Supplementary data associated with this article can be found, in the online version, at <http://dx.doi.org/10.1016/j.agrformet.2017.05.011>.

## References

- Anderson, J.T., Inouye, D.W., McKinney, A.M., Colautti, R.I., Mitchell-Olds, T., 2012. Phenotypic plasticity and adaptive evolution contribute to advancing flowering phenology in response to climate change. *Proc. R. Soc. B Biol. Sci.* 279, 3843–3852.
- Baskin, J.M., Baskin, C., 2004. A classification system for seed dormancy. *Seed Sci. Res.* 14, 1–16.
- Basler, D., 2016. Evaluating phenological models for the prediction of leaf-out dates in six temperate tree species across central Europe. *Agric. For. Meteorol.* 217, 10–21.
- Basler, D., Körner, C., 2012. Photoperiod sensitivity of bud burst in 14 temperate forest tree species. *Agric. For. Meteorol.* 165, 73–81.
- Basler, D., Körner, C., 2014. Photoperiod and temperature responses of bud swelling and bud burst in four temperate forest tree species. *Tree Physiol.* 34, 377–388.
- Berteaux, D., Reale, D., McAdam, A., Boutin, S., 2004. Keeping pace with fast climate

- change: can arctic life count on evolution? *Integr. Comp. Biol.* 44, 140–151.
- Burghardt, L.T., Metcalf, C.J.E., Wilczek, A.M., Schmitt, J., Donohue, K., 2015. Modeling the influence of genetic and environmental variation on the expression of plant life cycles across landscapes. *Am. Nat.* 185, 212–227.
- Caffarra, A., 2007. Quantifying the Environmental Drive of Tree Phenology. School of Natural Sciences, Trinity College, University of Dublin (Thesis).
- Caffarra, A., Donnelly, A., 2011. The ecological significance of phenology in four different tree species: effects of light and temperature on bud burst. *Int. J. Biometeorol.* 55, 711–721.
- Caffarra, A., Donnelly, A., Chuine, I., 2011. Modelling the timing of *Betula pubescens* budburst. II. Integrating complex effects of photoperiod into process-based models. *Clim. Res.* 46, 159–170.
- Chen, W., Black, T., Yang, P., Barr, A., Neumann, H., Nesic, Z., Blanken, P., Novak, M., Eley, J., Ketter, R., Cuenca, A., 1999. Effects of climatic variability on the annual carbon sequestration by a boreal aspen forest. *Global Change Biol.* 5, 41–53.
- Chuine, I., Beaubien, E., 2001. Phenology is a major determinant of tree species range. *Ecol. Lett.* 4, 500–510.
- Chuine, I., Bonhomme, M., Legave, J.M., Garcia de Cortazar, A., Charrier, G., Lacoine, A., Améglio, T., 2016. Can phenological models predict tree phenology accurately in the future? The unrevealed hurdle of endodormancy break. *Global Change Biol.* 22, 3444–3460.
- Chuine, I., Cour, P., Rousseau, D., 1998. Fitting models predicting dates of flowering of temperate-zone trees using simulated annealing. *Plant Cell Environ.* 21, 455–466.
- Chuine, I., Cour, P., Rousseau, D., 1999. Selecting models to predict the timing of flowering of temperate trees: implications for tree phenology modelling. *Plant Cell Environ.* 22, 1–13.
- Chuine, I., Garcia de Cortazar, A., Kramer, K., Hanninen, H., 2013. Development models. Phenology: An Integrative Environmental Science. Springer, Dordrecht, The Netherlands, pp. 275–293.
- Chuine, I., Morin, X., Bugmann, H., 2010. Warming, photoperiods, and tree phenology. *Science* 329, 277–278.
- Cooke, J.E.K., Eriksson, M.E., Junntila, O., 2012. The dynamic nature of bud dormancy in trees: environmental control and molecular mechanisms. *Plant Cell Environ.* 35, 1707–1728.
- Dantec, C.F., Vitasse, Y., Bonhomme, M., Louvet, J.M., Kremer, A., Delzon, S., 2014. Chilling and heat requirements for leaf unfolding in European beech and sessile oak populations at the southern limit of their distribution range. *Int. J. Biometeorol.* 58, 1853–1864.
- Delzon, S., Urli, M., Samalens, J.C., Lamy, J.B., Lischke, H., Sin, F., Zimmermann, N.E., Porte, A.J., 2013. Field evidence of colonisation by Holm Oak, at the Northern Margin of its distribution range, during the anthropocene period. *PLoS ONE* 8.
- Franks, S.J., Weber, J.J., Aitken, S.N., 2014. Evolutionary and plastic responses to climate change in terrestrial plant populations. *Evol. Appl.* 7, 123–139.
- Fu, Y.H., Liu, Y., De Boeck, H.J., Menzel, A., Nijs, I., Peaucelle, M., Penuelas, J., Piao, S., Janssens, I.A., 2016. Three times greater weight of daytime than of night-time temperature on leaf unfolding phenology in temperate trees. *New Phytol.* 212, 590–597.
- Fu, Y.H., Piao, S., Vitasse, Y., Zhao, H., De Boeck, H.J., Liu, Q., Yang, H., Weber, U., Hanninen, H., Janssens, I.A., 2015a. Increased heat requirement for leaf flushing in temperate woody species over 1980–2012: effects of chilling, precipitation and insolation. *Global Change Biol.* 21, 2687–2697.
- Fu, Y.H., Zhao, H., Piao, S., Peaucelle, M., Peng, S., Zhou, G., Ciais, P., Huang, M., Menzel, A., Uelas, J.P., Song, Y., Vitasse, Y., Zeng, Z., Janssens, I.A., 2015b. Declining global warming effects on the phenology of spring leaf unfolding. *Nature* 526, 104+.
- Hänninen, H., 1990. Modelling bud dormancy release in trees from cool and temperate regions. *Acta For. Fenn.* 213.
- Hanninen, H., Hakkinen, R., Hari, P., Koski, V., 1990. Timing of growth cessation in relation to climatic adaptation of northern woody-plants. *Tree Physiol.* 6, 29–39.
- Heide, O.M., 1993. Daylength and thermal time responses of budburst during dormancy release in some northern deciduous trees. *Physiol. Plant.* 88, 531–540.
- Heide, O.M., Prestrud, A.K., 2005. Low temperature, but not photoperiod, controls growth cessation and dormancy induction and release in apple and pear. *Tree Physiol.* 25, 109–114.
- Howe, G., Aitken, S., Neale, D., Jermstad, K., Wheeler, N., Chen, T., 2003. From genotype to phenotype: unraveling the complexities of cold adaptation in forest trees. *Can. J. Bot.* 81, 1247–1266.
- Howe, G., Davis, J., Jeknic, Z., Chen, T., Frewen, B., Bradshaw, H., Saruul, P., 1999. Physiological and genetic approaches to studying endodormancy-related traits in *Populus*. *Hortscience* 34, 1174–1184.
- Körner, C., Basler, D., 2010. Phenology under global warming. *Science* 327, 1461–1462.
- Kramer, K., 1994. Selecting a model to predict the onset of growth of *Fagus sylvatica*. *J. Appl. Ecol.* 31, 172–181.
- Lang, G., Early, J., Martin, G., Darnell, R., 1987. Endo-, para-, and ecodormancy: physiological terminology and classification for dormancy research. *HortScience* 22, 371–377.
- Lange, M., Schaber, J.A.M., Jäckel, G., Badeck, F., Seppelt, R., Doktor, D., 2016. Simulation of forest tree species bud burst dates for different climate scenarios: chilling requirements and photo-period may limit bud burst advancement. *Int. J. Biometeorol.* 60, 1711–1726.
- Laube, J., Sparks, T.H., Estrella, N., Hoefler, J., Ankerst, D.P., Menzel, A., 2014. Chilling outweighs photoperiod in preventing precocious spring development. *Global Change Biol.* 20, 170–182.
- Leinonen, I., Kramer, K., 2002. Applications of phenological models to predict the future carbon sequestration potential of boreal forests. *Clim. Change* 55, 99–113.
- Linkosalo, T., Hakkinen, R., Hanninen, H., 2006. Models of the spring phenology of boreal and temperate trees: is there something missing? *Tree Physiol.* 26, 1165–1172.
- Masle, J., Doussinault, G., Farquhar, G., Sun, B., 1989. Foliar stage in wheat correlates better to photothermal time than to thermal time. *Plant Cell Environ.* 12, 235–247.
- Meier, U., 2001. Growth Stages of Mono- and Dicotyledonous Plants. Wissenschafts-Verlag, Berlin pp. 158.
- Menzel, A., Sparks, T.H., Estrella, N., Koch, E., Aasa, A., Ahas, R., Alm-Kuebler, K., Bissolli, P., Braslavská, O., Briede, A., Chmielewski, F.M., Crepinsek, Z., Curnel, Y., Dahl, A., Defila, C., Donnelly, A., Filella, Y., Jatcza, K., Mage, F., Mestre, A., Nordli, O., Penuelas, J., Pirinen, P., Remisova, V., Scheifinger, H., Striz, M., Susnik, A., Van Vliet, A.J.H., Wielgolaski, F.E., Zach, S., Züst, A., 2006. European phenological response to climate change matches the warming pattern. *Global Change Biol.* 12, 1969–1976.
- Morin, X., Lechowicz, M.J., Augspurger, C., O'Keefe, J., Viner, D., Chuine, I., 2009. Leaf phenology in 22 North American tree species during the 21st century. *Global Change Biol.* 15, 961–975.
- Morin, X., Viner, D., Chuine, I., 2008. Tree species range shifts at a continental scale: new predictive insights from a process-based model. *J. Ecol.* 96, 784–794.
- Nathan, R., Horvitz, N., He, Y., Kuparinen, A., Schurr, F.M., Katul, G.G., 2011. Spread of North American wind-dispersed trees in future environments. *Ecol. Lett.* 14, 211–219.
- Piao, S., Ciais, P., Friedlingstein, P., Peylin, P., Reichstein, M., Luysaert, S., Margolis, H., Fang, J., Barr, A., Chen, A., Grelle, A., Hollinger, D.Y., Laurila, T., Lindroth, A., Richardson, A.D., Vesala, T., 2008. Net carbon dioxide losses of northern ecosystems in response to autumn warming. *Nature* 451, 49–52.
- Pope, K.S., Da Silva, D., Brown, P.H., DeJong, T.M., 2014. A biologically based approach to modeling spring phenology in temperate deciduous trees. *Agric. For. Meteorol.* 198, 15–23.
- Robertson, G.W., 1968. A biometeorological time scale for a cereal crop involving day and night temperatures and photoperiod. *Int. J. Biometeorol.* 12, 191–223.
- Root, T., Price, J., Hall, K., Schneider, S., Rosenzweig, C., Pounds, J., 2003. Fingerprints of global warming on wild animals and plants. *Nature* 421, 57–60.
- Saltre, F., Duputie, A., Gaucherel, C., Chuine, I., 2015. How climate, migration ability and habitat fragmentation affect the projected future distribution of European beech. *Global Change Biol.* 21, 897–910.
- Savolainen, O., Pyhajarvi, T., Knurr, T., 2007. Gene flow and local adaptation in trees. *Ann. Rev. Ecol. Evol. Syst.* 38, 595–619.
- Schaber, J., Badeck, F., 2003. Physiology-based phenology models for forest tree species in Germany. *Int. J. Biometeorol.* 47, 193–201.
- Vitasse, Y., Basler, D., 2013. What role for photoperiod in the bud burst phenology of European beech. *Eur. J. For. Res.* 132, 1–8.
- Vitasse, Y., Basler, D., 2014. Is the use of cuttings a good proxy to explore phenological responses of temperate forests in warming and photoperiod experiments? *Tree Physiol.* 34, 174–183.
- Vitasse, Y., Francois, C., Delpierre, N., Dufrene, E., Kremer, A., Chuine, I., Delzon, S., 2011. Assessing the effects of climate change on the phenology of European temperate trees. *Agric. For. Meteorol.* 151, 969–980.
- Vitasse, Y., Porte, A.J., Kremer, A., Michalet, R., Delzon, S., 2009. Responses of canopy duration to temperature changes in four temperate tree species: relative contributions of spring and autumn leaf phenology. *Oecologia* 161, 187–198.
- Way, D.A., Montgomery, R.A., 2015. Photoperiod constraints on tree phenology, performance and migration in a warming world. *Plant Cell Environ.* 38, 1725–1736.
- Zohner, C., Renner, S., 2015. Perception of photoperiod in individual buds of mature trees regulates leaf-out. *New Phytol.* 208 (4), 1023–1030.
- Zohner, C.M., Benito, B.M., Svenning, J.C., Renner, S.S., 2016. Day length unlikely to constrain climate-driven shifts in leaf-out times of northern woody plants. *Nat. Clim. Change* 6, 1120+.